Angiology: Open Access
ISSN: 2329-9495

Yang et al,. Angiol 2015, 3:2
DOI: 10.4172/2329-9495.1000149

Research Article Open Access

The Evaluation of Dual-Energy Myocardial Perfusion Imaging for the Detection of Acute Myocardial Infarction by Using the Second Generation Dual-Source CT in a Porcine Model

Xinchun Yang[1]*, Ruijuan Han[1], Kai Sun[2], Shuancheng Bai[2], Junyan Wang[2], Zhihui Liu[2], Guorong Liu[3],Yuechun Li[3], Kuncheng Li[4], Wenhuan Li[4], Yaojun Lu[5] and Ruiping Zhao[5]

[1]*Department of Cardiology, Chaoyang Hospital, Capital Medical University, Beijing 100020, China*
[2]*Department of Radiology, Baotou Central Hospital, Inner Mongolia, Baotou 014040, China*
[3]*Department of Neurology, Baotou Central Hospital, Inner Mongolia, Baotou 014040, China*
[4]*Department of Radiology, Xuanwu Hospital, Capital Medical University, Beijing 100053, China*
[5]*Department of Cardiology, Baotou Central Hospital, Inner Mongolia, Baotou 014040, China*

Abstract

Objectives: To evaluate the diagnostic accuracy of "one-step" dual-energy combined coronary CT angiography and first-pass myocardial perfusion imaging for the detection of acute myocardial infarction by using the second generation dual-source CT compared with conventional digital subtraction angiography and histopathological findings in a porcine model.

Methods: Five minipigs underwent transcatheter embolization of coronary using gelatin sponge to produce acute myocardial infarction. Arterial-phase myocardial DECT imaging were performed prior to and immediately and 24 hours after the procedure. A colour-coded iodine map was used for evaluation of myocardial perfusion defect using the 17-segment model. Two radiologists in consensus interpreted all iodine map imaging studies at DECT and coronary CT angiography images that were acquired during the DECT-acquisition. Statistical analysis for diagnostic accuracy was performed.

Results: Following the coronary embolization, DECT iodine maps showed 45 infarcted segments and 40 non infarcted segments. Based on the per-segment analysis, the sensitivity, specificity, positive predictive value and negative predictive value were 93%, 95%, 95% and 93%, respectively. The corresponding values to per-territory analysis were 100%, 86%, 89% and 100% using histopathological findings as the reference standard. The average dose length product (DLP) was 219.4 ± 60.9 mGy.cm (172-321 mGy.cm).

Conclusions: Our experimental study demonstrates that "one-step" dual-energy combined coronary CT angiography and first-pass myocardial perfusion imaging provides high diagnostic accuracy for detecting acute myocardial infarction and a comprehensive image quality of coronary artery with a relatively low dose of radiation in a porcine model.

Keywords: Computed tomography; Dual energy; Myocardial infarction; Heart perfusion

Introduction

Cardiac computed tomography (CT) has been shown a non-invasive tool with high diagnostic accuracy for the detection of coronary arterial stenosis [1]. However, the hemodynamic significance of many lesions is uncertain by Cardiac CT. Furthermore, the presence of calcified atherosclerotic plaque reduces the ability to differentiate significant stenosis from non-obstructive plaque. Thus, invasive angiography or perfusion imaging by single photon emission computed tomography (SPECT), positron emission tomography, or magnetic resonance imaging (MRI) are often better suited for accurately identifying obstructive or physiologically significant disease in these patients. Despite SPECT and PET can quantitatively determine myocardial blood flow (MBF) and coronary flow reserve, they often require high radiation dose exposure (9~11 mSv) and cannot evaluate coronary stenosis and cardiac structure due to its poor spatial resolution [1]. Although MRI requires no radiation and is accurate in identifying myocardial infarction [2], the technique requires longer time, and poses a problem in patients with pacemaker or defibrillator [3]. Extensive data regarding the prognostic value of myocardial perfusion imaging (MPI) have shown that the amount of infarcted and ischemic burden correlates with long-term outcomes and can help decide which patients are best suited for revascularization versus medical therapy. It follows that the ability to combine anatomical data from CT angiography together with the physiological significance provided by perfusion may be beneficial [4]. Dual-source CT (Dual Source Computed Tomography, DSCT) has two sets of X-ray tube as well as two sets of detectors, which allows dual energy CT (DECT) imaging and can differentiate different tissues or organs in the body according to the different intravascular iodine spectrum signals by various levels of X-ray penetration [5]. Different attenuation of different materials found inside the human body due to chemical composition and hence different kV settings (high and low); physical density of tissues and matter (how much of a certain material is there). For iodine, it is very specific dual-energy behavior, hence very well suited for DECT. This feature of DSCT provides

***Corresponding author:** Xinchun Yang, Department of Cardiology, Chaoyang Hospital, Capital Medical University, Beijing 100020, China, Tel: +86 013701186229; E-mail: YXC6229@163.com

Received May 20, 2015; **Accepted** June 26, 2015; **Published** June 30, 2015

Citation: Yang X, Han R, Sun K, Bai S, Wang J, et al. (2015) The Evaluation of Dual-Energy Myocardial Perfusion Imaging for the Detection of Acute Myocardial Infarction by Using the Second Generation Dual-Source CT in a Porcine Model. Angiol 3: 149. doi:10.4172/2329-9495.1000149

information for intra myocardial iodide signal distribution, which can reflect the myocardial perfusion, e.g. myocardial blood volume [6-8]. Preliminary animal and clinical studies have shown that DECT can provide a one-stop imaging that offers information about the coronary morphology as well as the myocardial blood supply, and that the results obtained through DECT is highly consistent with those by invasive coronary angiography (ICA), SPECT and MPI [8-15]. Compared to the 1st-generation DSCT, the second-generation DSCT (SOMATOM Definition Flash) demonstrate three major technological advances: expanded field of view (FOV), scanning with larger pitch and addition of Spectrum Photon Shield (SPS) on the high-energy CT Tubes. However, there is thus far very limited literature regarding utilization of 2nd-generation DSCT for evaluating myocardial perfusion reported by Weininger et al. [16] using MRI as comparison. To our knowledge, there were few studies to evaluate the diagnostic accuracy of 2nd generation dual-source CT using dual-energy myocardial perfusion imaging（DE-MPI for the detection of acute myocardial infarction in a porcine model. In this study, we evaluated the diagnostic accuracy of "one-step" dual-energy combined coronary CT angiography and first-pass myocardial perfusion imaging for the detection of acute myocardial infarction by using the second generation dual-source CT compared with conventional digital subtraction angiography and histopathological findings in a porcine model.

Materials and Methods

Ethical statement

Our study protocol was approved by Capital Medical University Animal Care and Use Committee and performed according to the Guide for the Care and Use of Laboratory Animals by the Association for Assessment and Accreditation of Laboratory Animal Care International.

Animal model

Total 5 porcines (Taihe Biotechnology Co, Ltd, Taizhou, Jiangsu, China, 25-34 kg) were enrolled in this study. All examinations were performed under general anesthesia and during continuous electrocardiogram monitoring. The porcines were anesthetized by the administration of an intramuscular injection consisting of 6 mg/kg Ketamine (6 mg/kg, Fujian Gutian Pharmaceutical Co, Ltd, Fujian, and China), midazolam (0.2 mg/kg, Jiangsu Enhua Pharmaceutical Group Co, Ltd, Jiangsu, China) and Penehyclidine Hydrochloride (1 mg, Chengdu Lisi Pharmaceutical Co, Ltd. Chenddu, China). An intravenous injection of 3.5 mg/kg propofol was then administered to all pigs. Anesthesia was maintained by a continuous intravenous injection of 6-8 mg/kg/h propofol. This protocol was used for the induction of MI as well as for the final CT examinations. During the acquisition of dual-energy CT dataset, esmolol hydrochloride injection (Qilu Pharmaceutical Co, Ltd, Shandong, China) was administrated continuously at a rate of 0.15 mg/kg·min to 0.3 mg/kg·min for heart rate reduction.

Induction of MI

Induction of MI was performed under the guidance of selective coronary angiography using gelatin sponge emboli. A 6F introducer sheath was inserted in one of femoral artery, and 10000 IU of heparin (Changzhou Pharmaceutical Co, Ltd, Jiangsu, and China) was administered. Additional 1000 IU heparin was injected per hour afterwards. A 5-French guiding catheter (Medtronic, Ltd, USA) was inserted into the lumen of the left coronary artery or right coronary artery through the introducer sheath. The guide wire was placed between the first and second diagonal branch of the LAD or the middle of the right coronary artery. Following the guide wire, a 3-French balloon (2.0 mm × 20 mm, Medtronic Co, Ltd, USA) was then placed at the distal end of the 2nd diagonal point of LAD or the middle of the right coronary artery. Balloon was open for pre-conditioning for 3-4 times, blocking the blood flow for 1 min, 2 min and 5 min, respectively, with 60 second interval. Gelatin sponge embolus (1.5 mm × 1.5 mm) was then placed by injection to the middle position of LAD or the middle position of RCA randomly and the vessel was temporarily occluded. In case of ventricular fibrillation during balloon occlusion, immediate defibrillation was performed. Subsequently, pigs were fed for 24 hours with special diet with high protein feed and plenty of water to put liquid back body due to blood loss during the procedure of induction of MI.

Scan Protocols and image reconstruction

All pigs were examined using a retrospective ECG-gated dual-energy mode with the 2nd-generation 128-slice DSCT (Definition Flash, Siemens Healthcare, Forchheim, Germany). Arterial-phase myocardial DECT imaging were performed prior to and immediately and 24 hours after the induction of MI. Dual-energy mode CT acquisition was obtained with the following characteristics: 280 ms gantry rotation time, pitch of 0.17 for spiral modes, collimation 2×64×0.6 mm/2×128×0.6 mm by means of a z-flying focal spot, tube current time 150 mAs/rot at Sn140 kVp and 165 mAs/rot at 100 kVp. A total of 1.5 mL/kg body-weight contrast agent iohexol (Omnipaque 350, 350 mg/mL, GE Healthcare, USA) was intravenously injected at 4 mL/s and followed by a 40 mL saline chaser bolus. Contrast-agent application was controlled using the bolus-tracking technique in the ascending aorta (signal attenuation threshold, 100 HU). Data acquisition was initiated after threshold was reached in the ascending aorta, with a mean delay of 4 seconds.

A single detector images at 100 kV with 140 ms temporal resolution protocol raw data for reconstruction was used did you use for coronary artery evaluation. CT Angiographic images were reconstructed in a standard way using retrospective ECG-gating and single-segment reconstruction in best diastolic phase when HR≤70 bpm or best systolic when HR>70 bpm (Best Phase, Siemens Healthcare, Forchheim, Germany) with a slice thickness of 0.75 mm with an increment of 0.4 mm, and a medium-soft convolution kernel (B26f). For the evaluation of myocardial iodine content, images from the same raw data set were then automatically reconstructed into 3 image datasets (100 kVp, 140 kVp, and an average weighted image set, M_0.3) merging 70% of the 100 kVp and 30% of the 140 kVp information). The average weighted images were weighted fused images with 1.0 mm slice thickness and 0.75 mm intervals using a D30 dual energy cardiac kernel. Further post-processing was performed on a commercially available workstation (Syngo MMWP, VA36, Siemens Healthcare, Forchheim, Germany) using the dedicated dual-energy heart-PBV application to obtain myocardial "iodine maps" in the short axis, long axis, and 4 chamber views. These iodine maps, which represent the myocardial blood pool, were 16-bit color-coded and then superimposed onto the grayscale anatomic multiplanar reformations of the myocardium. The resulting color-coded "iodine maps"were then superimposed on gray-scale multiplanar reformats of the virtual non enhanced data sets of the myocardium in short- and long-axis views of the left ventricle. Color coding was performed using shades of green ("PET" template) with bright green coding for high iodine content and black coding for a complete lack of iodine. For image analysis, the iodine maps were superimposed as a 60% overlay onto the grayscale multiplanar reformats with a slice thickness of 1.5 mm. Curved planar reformatting

(CPR) (thickness 8.0 mm), maximum intensity projection (MIP) (thickness 10.0 mm), multiplanar reformatting (MPR) and volume rendering (VR) were used to evaluate the coronary arteries.

Image interpretation

Two additional radiologists, experienced in the field of cardiac imaging (3 and 5 years of experience) and blinded to the corresponding histopathology findings, independently analyzed all three reconstructed DECT series in random order and blinded to the used reconstruction method. Sensitivity, specificity, positive predictive value (PPV), negative predictive value (NPV), and accuracy for the detection of MI were calculated for each imaging modality on a segment basis according to the American Heart Association (AHA) 17-segment model, using histopathology findings as standard of reference. Coronary segments were defined according to standards of the AHA standards: segments 1 to 4 included the right coronary artery (RCA), segment 5 included the left main artery (LM), segments 6 to 10 included the left anterior descending artery (LAD), segments 11 to 15 included the left circumflex artery (LCX), and segment 16 included the intermediary artery. The qualities of images of the coronary were rated on a 4-point scale [17] as follows: 1= excellent, no artifacts; 2=good, mild artifacts, unrestricted evaluation; 3= evaluable, moderate artifacts but still diagnostic combined with axial images; 4 = unevaluable, severe artifacts leading to no diagnostic images on a per-segment basis [18]. Radiation dose: the dose length product (dose length product, DLP) was automatically calculated by the CT.

Histopathology

Histopathology was regarded as the standard of reference in this study. Immediately after DECT, all pigs were killed and the hearts excised and processed by washing with water and freezing in -20°C for 60 min. Along the short axis, left ventricle were sectioned at thickness of 3 mm, flat immersed in 1% triphenyltetrazolium chloride (TTC) solution and then stained at 37°C for 1 hour for histopathological analysis. Tissues from central and surrounding regions of infarction as well as normal myocardial tissues were collected for after he staining and pathological examination to confirm the presence or absence of myocardial infarction.

Statistical analysis

Statistical analysis was performed using SPSS 19.0 (SPSS, Chicago, IL, USA). Measurement data were presented as mean ± SD. Using the pathological findings as the reference standard, the sensitivity, specificity and positive and negative predictive values of DECT for detecting myocardial perfusion defect segments were calculated. Consistency analysis between different observers was performed using Cohen's Kappa analysis (kappa> 0.81: excellent consistency; kappa = 0.61-0.80: good consistency; kappa = 0.41-0.60: medium consistency; kappa = 0.21-0.40: fair consistency; kappa <0.20: poor consistency).

Results

Myocardial infarction models were successfully established in all pigs, one of which had a distal occlusion of the right coronary artery, two had occlusions in the middle segment of LAD plus the proximal circumflex artery and two had occlusions only in the middle segment of LAD. Two pigs presented ventricular tachycardia during the process of occlusion in LAD and recovered after intravenous injection of lidocaine immediately. The average weight of pigs were 29 ± 3.8 (25 ~ 34) kg.

The inter-observer agreement in the assessment of myocardial perfusion iodine map was good (kappa=0.74). Based on the iodine map segmental analysis, DECT myocardial perfusion evaluated 85 myocardial segments totally, 45 of which were identified to be blood pool deficit and 40 to be normal blood pool myocardial segments. Regarding pathological findings as the reference standard, 43 segments identified by DECT were confirmed to have infarction with 2 segments as a false positive and 3 segments as false negative, respectively. Representative results of the true-positive and true-negative of dual-energy combined coronary CT angiography and myocardial perfusion imaging are shown in (Figure 1). False-positive and false-negative of dual-energy myocardial perfusion imaging are shown in (Figure 2).

When the analyses were performed according to the vascular distribution regions, a total of 15 regions were evaluated, including 9 with blood pool defect and 6 normal regions. Compared to the pathological findings, there were 2 myocardial segments were falsely evaluated positive (myocardial segments 13,14) and 3 myocardial segments of falsely rated as negative (myocardial segments 14,15,16) and only one region identified by DECT was confirmed to be false positive and no false negative was found (Table 1) details the comparative results of DECT and histopathological detections of myocardial infarction in terms of regions and numbers of ischemic segments. Sensitivity, specificity, positive predictive value, negative predictive values for DECT detection of myocardial perfusion is shown in (Table 2).

TTC staining of normal myocardium is red and ischemic myocardium is white. Histopathological analysis identified a total of 46 segments of myocardial infarction and 39 normal myocardial segments. HE staining show infarcted myocardium lesions and normal myocardial foci interspersely arranged which is visible at low magnification microscope. When visualized under high magnification microscope, pathological changes such as myocardial cytoplasm

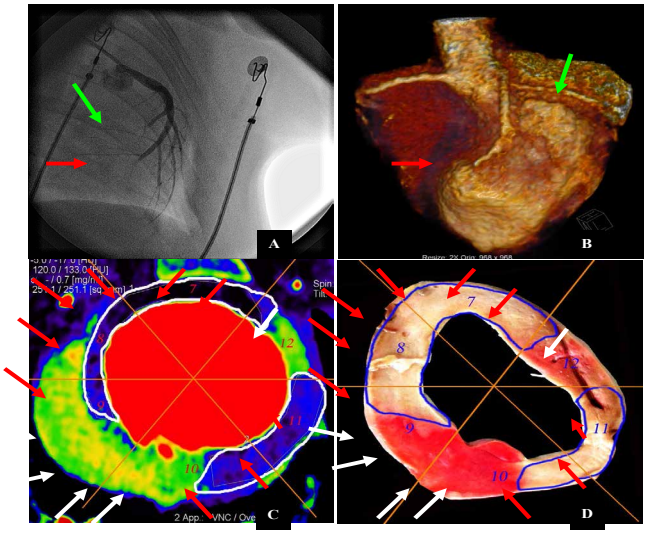

Figure 1: Representative results of the true-positive and true-negative of dual-energy combined coronary CT angiography and myocardial perfusion imaging. Invasive angiography (A) confirms obstruction in the middle of left anterior descending artery (red arrow) and left circumflex artery (green arrow). Coronary CT angiography demonstrated the obstruction (B). Dual-energy iodine imaging (C) presented the blood pool deficit in the myocardial segments 7,8,9,10,11 (red arrow) and the corresponding myocardial infarction segments (red arrow) presented in the triphenyltetrazolium chloride (TTC) pathology (D). While the myocardial segments 9,10,12 (C) (white arrow) presented normal blood pool and corresponding normal myocardial infarction myocardial segments (white arrow) in the pathology (D).

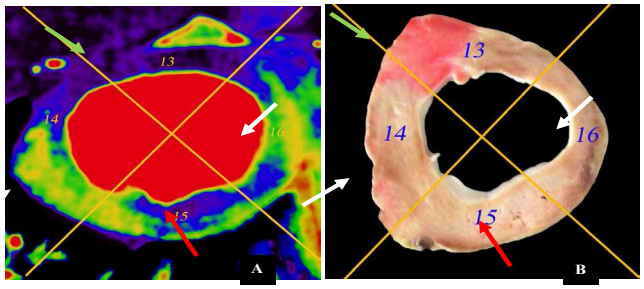

Figure 2: False-positive and false-negative of dual-energy myocardial perfusion imaging. Dual-energy iodine imaging (A) presented the blood pool deficit in the myocardial segments 13 (green arrow) which was confirmed normal myocardial segments (green arrow) in the triphenyltetrazolium chloride (TTC) pathology (B) (false-positive). Dual-energy iodine imaging (A) presented the normal blood pool in the myocardial segments 14,16 (white arrow) which was presented myocardial infarction segments (white arrow) in the triphenyltetrazolium chloride (TTC) pathology (D) (false-negative).

cohesion, eosinophilic change, disappearance of stripes, nucleus relocation and myocardial cell interstitial edema were all observed; some severely damaged myocardial cells demonstrate disappearance of nucleus and basophilic granules.

The average heart rates were 102 ± 18 (80~128) bpm. In our experimental porcine study, even with the intravenous administration of a high dose of esmolol hydrochloride were used to reduce heart rate, we were unable to obtain a low heart rate even two cases above 100 bpm which maybe have a strong negative effect on image quality for all coronary segments and each coronary artery. A total of 56 coronary segments were displayed. For 2 pigs with heart rate above 100 bpm (110 bpm and 128 bpm, respectively), their coronary images quality were poor. The coronary segments images met the diagnostic requirements and the average score was 1.1 ± 0.4 for pigs with heart rate ≤100 bpm. However, for pigs with heart rate > 100 bpm, their coronary segments images are poor and the average score was 3.9 ± 0.3. Coronary image quality scores are shown in (Table 3). The average DLP was 219.4 ± 60.9 mGy.cm (172 ~ 321 mGy.cm).

Discussion

Our results demonstrate a sensitivity of 93% and a specificity of 95% for detecting acute myocardial infarction by using the dual-energy single contrast-enhanced myocardial perfusion imaging with 2nd generation dual-source CT, compared with histopathological findings in a porcine model. This "One-step" dual-energy combined coronary CT angiography and myocardial perfusion protocol provides a comprehensive image quality of coronary artery.

The differentiation of viable from infarcted myocardium is important to predict an improvement in the left ventricular function, detect occult infarcts and to identify the risk for future cardiac events. However, infarcted segments may be difficult to identify at CT, especially where the SNR ratio is low or the infarct size is small. Using these two energy spectra DECT exploits the fact that tissues in the human body and the intravascular iodine-based contrast material could be used to enable the mapping of iodine (and thus blood) distribution within the myocardium as a stand-in of myocardial blood volume. DECT therefore uses the opportunity of material differentiation of DSCT in dual energy mode to show myocardial areas of decreased contrast material content. Previous reports showed that the accuracy for the 1st-generation dual-source, dual-energy myocardial perfusion CT to detect myocardial ischemia / infarction can vary, from 72-93% for sensitivity and 72-94% for the specificity [10-13, 9]. The second-generation DSCT is equipped with an additional tin filter which hardens the high-energy spectrum (then denoted as Sn140 kVp). This filter absorbs the low-energy photons thus reducing radiation dose and decreasing the spectral overlap between low- and high-energy spectra, which has been shown to allow for a more accurate material decomposition which is likely to translate into more accurate iodine quantification [19]. This agrees well with our findings of the high diagnostic accuracy with second-generation DSCT compared to the report of the first-generation DSCT.

In our study, DECT were confirmed to have with infarction with 2 segments as a false positive and 3 segments as false negative, respectively. The reason of false positive of dual-energy myocardial perfusion was the irreversibly damaged infarcted myocardium and hibernating myocardium were both presented as the blood pool deficit of myocardial segments in iodine imaging .Hibernating myocardium is considered to be myocardium with diminished contractility due to reduced perfusion because of severe coronary artery stenosis. Deseive et al. [20] demonstrated that infarcted myocardium showed a higher concentration of iodine than normal myocardium in the late enhancement phase. However, we only focused on the detection of acute myocardial infarction in a single-phase scan. We think this is a reason of false positive and a limitation of our study.

Methods	Myocardial segments																	Total
	1	2	3	4	5	6	7	8	9	10	11	12	13	14	15	16	17	
DECT Iodine	2	2	1	2	2	0	4	4	4	1	4	0	4	4	4	3	4	45
Histopathology	2	2	1	2	2	2	4	4	4	1	4	0	2	4	4	4	4	46

Table 1: Segmental region and number of myocardial infarction detected by DECT and histopathology.

Diagnostic accuracy	Per-segment analysis (n=85)	Per-territory analysis (n=15)
True-positive	40	8
False-positive	2	1
True-negative	40	6
False-negative	3	0
Sensitivity (%) (95% CI)	93 (81% - 98%)	100 (63% - 100%)
Specificity (%) (95% CI)	95% (83% - 99%)	86% (42% - 97%)
Positive predictive value (%) (95% CI)	95% (83% - 99%)	89% (52% - 98%)
Negative predictive value (%) (95% CI)	93 (81% - 98%)	100 (54% - 100%)

Table 2: Accuracy assessment for DECT Iodine map detection of myocardial infarction.

Coronary Segments	RCA 1 2 3 4				LM 5	LAD 6 7 8 9 10					CX 11 12 13 14 15					IA 16
HR≤100bpm Segment number	3	3	3	3	3	3	3	3	1	1	3	2	3	1	1	0
Score 1	3	1	2	3	3	3	3	3	1	1	3	2	3	1	1	0
Score 2	0	1	0	0	0	0	0	0	0	0	0	0	0	0	0	0
Score 3	0	1	1	0	0	0	0	0	0	0	0	0	0	0	0	0
Score 4	0	0	0	0	0	0	0	0	0	0	0	0	0	0	0	0
HR>100bpm Segment number	2	2	2	2	2	2	2	0	0	0	2	2	2	0	0	0
Score 1	0	0	0	0	0	0	0	0	0	0	0	0	0	0	0	0
Score 2	0	0	0	0	0	0	0	0	0	0	0	0	0	0	0	0
Score 3	0	0	0	0	0	1	1	0	0	0	0	0	0	0	0	0
Score 4	2	2	2	2	2	1	1	0	0	0	2	2	2	0	0	0

RCA = right coronary artery, LM = left main artery, LAD = left anterior descending artery, LCX = left circumflex artery, IA = Intermediate artery.

Table 3: Scoring of coronary artery image quality (scores: 1-4).

Regarding the image quality of coronary CTA by the dual-energy CT myocardial perfusion, previous reports have shown that the coronary CTA image acquired by the first generation DECT was not sufficient for diagnosis [11,13]. In our study, we assessed the quality of image acquired by the 2nd-generation DECT and found that the coronary segment images acquired from the pigs with heart rate ≤100 bpm can be used for diagnosis. These data suggest that the second-generation dual-source CT can acquire high quality image under low heart rates through a single enhanced scanning, which is related to the higher time resolution of tubes in the 2nd-generation DSCT. Finally, we also evaluated the radiation doses required by these different CT techniques. Ruzsics et al reported that effective radiation dose of DECT for a single scanning of myocardial perfusion in patients was 14 ± 5 mSv [7]. We here show that the mean radiation dose in our model using the 2nd-generation DSCT is 219.4 ± 60.9 mGy.cm, which is significantly lower than the first-generation dual-source CT reported in previous studies.

Study Limitations

This study has several limitations. First, we had a relatively small number of the animals in this study. Additional larger studies are warranted to fully assess the comparability of the results. Second, there was lack of inclusion of SPECT and MRI for parallel comparison. Future studies are warranted to further investigate this area. Third, our results using DECT were focused on the detection of healed infarction from a single-phase scan.

Conclusion

In conclusion, our experimental study demonstrates that "one-step" dual-energy combined coronary CT angiography and first-pass myocardial perfusion imaging provides high diagnostic accuracy for detecting acute myocardial infarction and a comprehensive image quality of coronary artery with a relatively low dose of radiation dose in a porcine model.

References

1. Carrascosa P, Capuñay C, Deviggiano A, Goldsmit A, Tajer C, et al. (2010) Accuracy of low-dose prospectively gated axial coronary CT angiography for the assessment of coronary artery stenosis in patients with stable heart rate. J Cardiovasc Comput Tomogr 4: 197-205.
2. Hartlage G, Janik M, Anadiotis A, Veledar E, Oshinski J, et al. (2012) Prognostic value of adenosine stress cardiovascular magnetic resonance and dobutamine stress echocardiography in patients with low-risk chest pain. Int J Cardiovasc Imaging 28: 803-812.
3. Srichai MB, Chandarana H, Donnino R, Lim II, Leidecker C, et al. (2013) Diagnostic accuracy of cardiac computed tomography angiography for myocardial infarction. World J Radiol 5: 295-303.
4. Kim SM, Choi JH, Chang SA, Choe YH (2013) Detection of ischaemic myocardial lesions with coronary CT angiography and adenosine-stress dynamic perfusion imaging using a 128-slice dual-source CT: diagnostic performance in comparison with cardiac MRI. Br J Radiol 86: 20130481.
5. Johnson TR, Krauss B, Sedlmair M, Grasruck M, Bruder H, et al. (2007) Material differentiation by dual energy CT: initial experience. Eur Radiol 17: 1510-1517.
6. Ruzsics B, Lee H, Powers ER, Flohr TG, Costello P, et al. (2008) Images in cardiovascular medicine. Myocardial ischemia diagnosed by dual-energy computed tomography: correlation with single-photon emission computed tomography. Circulation 117: 1244-1245.
7. Ruzsics B, Lee H, Zwerner PL, Gebregziabher M, Costello P, et al. (2008) Dual-energy CT of the heart for diagnosing coronary artery stenosis and myocardial ischemia-initial experience. Eur Radiol 18: 2414-2424.
8. Ruzsics B, Schwarz F, Schoepf UJ, Lee YS, Bastarrika G, et al. (2009) Comparison of dual-energy computed tomography of the heart with single photon emission computed tomography for assessment of coronary artery stenosis and of the myocardial blood supply. Am J Cardiol 104: 318-326.
9. Ko SM, Choi JW, Song MG, Shin JK, Chee HK, et al. (2011) Myocardial perfusion imaging using adenosine-induced stress dual-energy computed tomography of the heart: comparison with cardiac magnetic resonance imaging and conventional coronary angiography. Eur Radiol 21: 26-35.
10. Wang R, Yu W, Wang Y, He Y, Yang L, et al. (2011) Incremental value of dual-energy CT to coronary CT angiography for the detection of significant coronary stenosis: comparison with quantitative coronary angiography and single photon emission computed tomography. Int J Cardiovasc Imaging 27: 647-656.
11. Zhang LJ, Peng J, Wu SY, Yeh BM, Zhou CS, et al. (2010) Dual source dual-energy computed tomography of acute myocardial infarction: correlation with histopathologic findings in a canine model. Invest Radiol 45: 290-297.
12. Kerl JM, Deseive S, Tandi C, Kaiser C, Kettner M, et al. (2011) Dual energy CT for the assessment of reperfused chronic infarction - a feasibility study in a porcine model. Acta Radiol 52: 834-839.
13. Peng J, Zhang LJ, Schoepf UJ, Gibbs KP, Ji HS, et al. (2013) Acute myocardial infarct detection with dual energy CT: correlation with single photon emission computed tomography myocardial scintigraphy in a canine model. Acta Radiol 54: 259-266.
14. Feuchtner G, Goetti R, Plass A, Weiser M, Scheffel H, et al. (2011) Adenosine stress high-pitch 128-slice dual-source myocardial computed tomography perfusion for imaging of reversible myocardial ischemia: comparison with magnetic resonance imaging. Circ Cardiovasc Imaging 4: 540-549.
15. Rocha-Filho JA, Blankstein R, Shturman LD, Bezerra HG, Okada DR, et al. (2010) Incremental value of adenosine-induced stress myocardial perfusion imaging with dual-source CT at cardiac CT angiography. Radiology 254: 410-419.

16. Weininger M, Schoepf UJ, Ramachandra A, Fink C, Rowe GW, et al. (2012) Adenosine-stress dynamic real-time myocardial perfusion CT and adenosine-stress first-pass dual-energy myocardial perfusion CT for the assessment of acute chest pain: initial results. Eur J Radiol 81: 3703-3710.

17. Ghadri JR, Küest SM, Goetti R, Fiechter M, Pazhenkottil AP, et al. (2012) Image quality and radiation dose comparison of prospectively triggered low-dose CCTA: 128-slice dual-source high-pitch spiral versus 64-slice single-source sequential acquisition. Int J Cardiovasc Imaging 28: 1217-1225.

18. Korn A, Fenchel M, Bender B, Danz S, Thomas C, et al. (2013) High-pitch dual-source CT angiography of supra-aortic arteries: assessment of image quality and radiation dose. Neuroradiology 55: 423-430.

19. Koonce JD, Vliegenthart R, Schoepf UJ, Schmidt B, Wahlquist AE, et al. (2014) Accuracy of dual-energy computed tomography for the measurement of iodine concentration using cardiac CT protocols: validation in a phantom model. Eur Radiol 24: 512-518.

20. Deseive S, Bauer RW, Lehmann R, Kettner M, Kaiser C, et al. (2011) Dual-energy computed tomography for the detection of late enhancement in reperfused chronic infarction: a comparison to magnetic resonance imaging and histopathology in a porcine model. Invest Radiol 46: 450-456.

Citation: Yang X, Han R, Sun K, Bai S, Wang J, et al. (2015) The Evaluation of Dual-Energy Myocardial Perfusion Imaging for the Detection of Acute Myocardial Infarction by Using the Second Generation Dual-Source CT in a Porcine Model. Angiol 3: 149. doi:10.4172/2329-9495.1000149